

LTH 885

RI'/SMOM scheme amplitudes for deep inelastic scattering operators at one loop in QCD

J.A. Gracey,
Theoretical Physics Division,
Department of Mathematical Sciences,
University of Liverpool,
P.O. Box 147,
Liverpool,
L69 3BX,
United Kingdom.

Abstract. We compute the amplitudes for the insertion of various operators in a quark 2-point function at one loop in the RI' symmetric momentum scheme, RI'/SMOM. Specifically we focus on the moments $n = 2$ and 3 of the flavour non-singlet twist-2 operators used in deep inelastic scattering as these are required for lattice computations.

1 Introduction.

Lattice gauge theories are the main theoretical tool for exploring the non-perturbative régime of the strong nuclear force by simulating the underlying quantum field theory which is the non-abelian gauge theory of quarks and gluon, (QCD). The numerical techniques allows one to explore the infrared region where perturbation theory becomes impractical because the value of the parameter controlling the expansion, which is the coupling constant, becomes large. Briefly, one uses the path integral formalism but with the space-time continuum replaced by a discrete Euclidean grid. Then one can construct Green's functions numerically, representing, for example, bound state particle spectra, and make measurements of the masses. Whilst overlooking many of the technical aspects of this procedure at this point, it is a remarkable achievement that the formalism is in more than solid agreement with nature. Aside from determining particle spectra, one of the current main problems is to measure matrix elements of operators in the non-perturbative region. These are important in, for instance, understanding the structure of nucleons if one focuses on the operators relating to deep inelastic scattering. These were introduced originally in [1] which subsequently produced an intense industry to determine the operator anomalous dimensions for arbitrary moment to eventually three loops in the $\overline{\text{MS}}$ renormalization scheme, [2, 3, 4, 5, 6, 7]. Indeed there has been a large degree of progress in the area of measuring matrix elements of quark bilinear currents and operators and the associated renormalization constants by the QCDSF collaboration, [8, 9, 10, 11, 12, 13, 14], and others [15, 16, 17, 18, 19, 20, 21, 22, 23, 24]. However, in order to make reliable measurements and hence accurate predictions one has to overcome various theoretical difficulties. Aside from those relating specifically to the lattice, there is the problem of ensuring the results match on to what would be expected at high energies. In other words the Green's function depends on some reference momentum value and the numerical simulations, in principle, make measurements not only at low but also at high energies. In the latter case perturbation theory is actually valid there and hence is a reliable complementary tool. Therefore, if the same Green's function is computed to several loop orders then it ought to be the case that the numerical measurements will overlap at large energies. Given this, it is sometimes the situation when there are accurate large loop order results that the continuum estimate is used to assist with normalizing the lattice measurements.

This brief overview clouds some of the more technical aspects of the overall procedure. For instance, all the operators of interest undergo renormalization. Whilst this is not a major problem, since the formalism to carry out a renormalization has been established for many years now, there is the problem of the relation of a continuum renormalization to what is performed in practice on the lattice. For instance, the standard practice in high energy problems is to dimensionally regularize QCD and then to subtract the resulting divergences, which are manifested as poles in the regularizing parameter ϵ , in a minimal or modified minimal way. The latter scheme, $\overline{\text{MS}}$, is the main procedure primarily as convergence is improved by removing a specific finite part in addition to the basic poles. The main advantage of this mass independent renormalization scheme is that one can compute to very high loop order when the quarks are massless and even to a reasonable order in some cases when there are massive quarks. Whilst this provides accurate results for the lattice to match to, there is the technical problem to be overcome which is that the lattice computations are invariably in a non-minimal renormalization scheme. So to make a proper comparison for matching at high energy one has to convert the results to the *same* scheme. One of the more widely used lattice schemes is the RI' scheme, [25, 26], which denotes the modified regularization invariant scheme. It is a modification of the RI scheme, [25, 26], where the essential difference is in the way the quark wave function renormalization constant is defined. Briefly, the difference between the RI' and RI schemes is in a differentiation of the quark 2-point function with respect to the momentum. As the derivative

has a financial cost for the lattice, the RI' scheme is more efficient and hence is the default scheme in this respect, [25, 26]. Both these lattice schemes are mass dependent renormalization schemes and are a hybrid of $\overline{\text{MS}}$ and MOM schemes. By this we mean that in the main 2-point functions are renormalized according to a MOM type subtraction whilst three and higher point functions are renormalized using $\overline{\text{MS}}$. This ensures, for example, that the RI and RI' scheme coupling constants are the same as that of the $\overline{\text{MS}}$ scheme, [25, 26]. Whilst introduced in [25, 26], the renormalization of QCD in the continuum has been studied in the Landau gauge in [27] and later in a general linear covariant gauge in [28].

Consequently, with interest in measuring matrix elements on the lattice relating to nucleon structure there has been a need to carry out the continuum RI' renormalization of the same Green's functions. These involve the low moment flavour non-singlet twist-2 Wilson operators which arise in the deep inelastic scattering formalism. Indeed three loop results are available in RI' in [28, 29, 30]. As these renormalization constants are determined by inserting the operator into a quark 2-point function with massless quarks then one could apply standard algorithms such as MINCER, [31, 32], to achieve high loop orders. However, from a technical point of view this renormalization is carried out at a point of exceptional momentum since the operator is inserted at zero momentum. In this configuration one is effectively dealing with a reduced 2-point function. It has recently been pointed out, [33], that for matrix elements relating to quark masses then one could have infrared issues in extracting reliable results in the non-perturbative region as a consequence of this momentum configuration. To circumvent this technicality an alternative scheme has been developed which is called the RI'/SMOM scheme, [33]. It differs from the RI' scheme in that 3-point functions are not subtracted at an exceptional point but instead at a symmetric point. This means that none of the external momenta are nullified, so that the potential infrared singularity embedded within the logarithms of the Green's function are bypassed, [33]. Whilst the one loop computations were performed in [33], this has recently been extended to two loops in [34, 35] for the scalar quark current. However, given that there is recent interest in measuring twist-2 flavour non-singlet operator matrix elements on the lattice for low moments, [23], it is the purpose of this article to present the first one loop computations for the moments $n = 2$ and 3 . Although lattice computations focus on the Landau gauge, partly as that gauge is less complicated to fix numerically, the Green's function with the operator insertion is gauge dependent. So in developing another renormalization scheme to overcome one technical problem there are potential numerical errors in measurements from gauge fixing issues. Instead all our results will be in a general linear covariant gauge. Whilst the renormalization of these Wilson operators has already been carried out for the RI' scheme, [28, 29, 30], it may appear to be rather simple to follow that procedure for the latest scheme. This is not the case for an elementary reason. This is to do with the fact that the Wilson operators mix under renormalization, [36]. It is widely accepted that the flavour singlet Wilson operators mix among themselves and the flavour non-singlet ones do not, [1, 2, 3]. Indeed in the original context of [1, 2, 3] this is the situation. However, that is only the case for the latter set if the Green's function containing the operator does not have a momentum flowing out of the operator itself. If there is a net momenta flow through the operator then they mix into a set of total derivative operators. Given that the RI'/SMOM scheme is at non-exceptional momenta then this mixing cannot be ignored. It has been studied to three loops in a practical situation in [36] where a similar problem for the lattice was examined but in a context which involves a Green's function which is gauge independent but contains two operators. Indeed the mixing matrix for the two operators we consider here was calculated to three loops in the $\overline{\text{MS}}$ scheme. Without including the mixing in [36] the operator correlation function did not correctly satisfy the renormalization group equation at two and three loops.

The article is organised as follows. We review the problem and the necessary background

in the following section. All our results are collected in section three where we give all the amplitudes as a function of the gauge parameter of an arbitrary linear covariant gauge. We conclude in section four and include an appendix. It contains the bases of tensors into which all the Green's functions are decomposed together with the coefficients of the projection tensors which project out each specific amplitude.

2 Preliminaries.

In this section we recall the background to the problem and the calculational set-up. First, the various operators we will be considering, which are gauge invariant, are

$$\begin{aligned}
S &\equiv \bar{\psi}\psi \\
V &\equiv \bar{\psi}\gamma^\mu\psi \\
T &\equiv \bar{\psi}\sigma^{\mu\nu}\psi \\
W_2 &\equiv \mathcal{S}\bar{\psi}\gamma^\mu D^\nu\psi \\
\partial W_2 &\equiv \mathcal{S}\partial^\mu(\bar{\psi}\gamma^\nu\psi) \\
W_3 &\equiv \mathcal{S}\bar{\psi}\gamma^\mu D^\nu D^\sigma\psi \\
\partial W_3 &\equiv \mathcal{S}\partial^\mu(\bar{\psi}\gamma^\nu D^\sigma\psi) \\
\partial\partial W_3 &\equiv \mathcal{S}\partial^\mu\partial^\nu(\bar{\psi}\gamma^\sigma\psi)
\end{aligned} \tag{2.1}$$

where the first three operators are included for checking purposes and all derivatives, both ordinary and covariant, act to the right. In (2.1) \mathcal{S} means total symmetrization in the free Lorentz indices and we use the same labelling and notation as [36] for ease of reference. For instance, at certain points in this respect we will refer to the level W_2 or W_3 . By this we will mean either the specific operator with that label or the set of operators within that level which are additionally either ∂W_2 or ∂W_3 and $\partial\partial W_3$ respectively. Like [36], it will be clear from the context which is meant. As discussed already one must include these additional total derivative operators within each level since there is mixing between the operators. Such mixings must be included when there is a momentum flowing through the operator insertion in the Green's function irrespective of the number of such included operators. For the earlier RI' scheme computations of the anomalous dimensions the mixing issue was not relevant since the operator was inserted at zero momentum, [28, 29, 30]. Given that we are considering operators with free Lorentz indices, whether they relate to deep inelastic scattering or not, we cannot follow the earlier prescription of [1, 2, 3]. There the free Lorentz indices of the matrix elements were contracted with a null vector, Δ_μ , which projected out that part of the matrix element containing the divergence. The reason that we have to take a different approach resides in the fact that on the lattice measurements are made for various individual components of the free indices. Therefore, we have to take a more general approach and decompose our Green's functions into a basis of Lorentz tensors which have the *same* symmetry structure as the operator which is inserted into the Green's function. For the tensor current this means that the basis has to be antisymmetric in the two free indices since $\sigma^{\mu\nu} = \frac{1}{2}[\gamma^\mu, \gamma^\nu]$. In the case of the two Wilson operators each operator in the respective levels are totally symmetric in the indices and are traceless in d -dimensions, [1]. To be specific we have

$$\begin{aligned}
\mathcal{S}\mathcal{O}_{\mu\nu}^{W_2} &= \mathcal{O}_{\mu\nu}^{W_2} + \mathcal{O}_{\nu\mu}^{W_2} - \frac{2}{d}\eta_{\mu\nu}\mathcal{O}_\sigma^{W_2\sigma}, \\
\mathcal{S}\mathcal{O}_{\mu\nu\sigma}^{W_3} &= \mathcal{O}_{S\mu\nu\sigma}^{W_3} - \frac{1}{(d+2)}\left[\eta_{\mu\nu}\mathcal{O}_{S\sigma\rho}^{W_3\sigma\rho} + \eta_{\nu\sigma}\mathcal{O}_{S\mu\rho}^{W_3\mu\rho} + \eta_{\sigma\mu}\mathcal{O}_{S\nu\rho}^{W_3\nu\rho}\right]
\end{aligned} \tag{2.2}$$

with

$$\mathcal{O}_{S\ \mu\nu\sigma}^{W_3} = \frac{1}{6} \left[\mathcal{O}_{\mu\nu\sigma}^{W_3} + \mathcal{O}_{\nu\sigma\mu}^{W_3} + \mathcal{O}_{\sigma\mu\nu}^{W_3} + \mathcal{O}_{\mu\sigma\nu}^{W_3} + \mathcal{O}_{\sigma\nu\mu}^{W_3} + \mathcal{O}_{\nu\mu\sigma}^{W_3} \right] \quad (2.3)$$

where the basic operators are

$$\begin{aligned} \mathcal{O}_{\mu\nu}^{W_2} &= \bar{\psi} \gamma_\mu D_\nu \psi, \\ \mathcal{O}_{\mu\nu\sigma}^{W_3} &= \bar{\psi} \gamma_\mu D_\nu D_\sigma \psi \end{aligned} \quad (2.4)$$

and D_μ is the usual covariant derivative. These are the same definitions as used in earlier computations, [28, 29, 30]. The total derivative operators in the same respective levels satisfy these same template definitions. (We have suppressed the free flavour indices but note that these are flavour non-singlet operators.)

Next we recall the key points concerning the mixing of the operators in levels W_2 and W_3 . First, as we are working with massless quarks there are no lower dimensional operators to be included and there is no mixing between levels. Next the particular choice of operators, (2.1), means that whilst there is mixing the mixing matrix of renormalization constants is upper triangular and given by, [36],

$$Z_{ij}^{W_2} = \begin{pmatrix} Z_{11}^{W_2} & Z_{12}^{W_2} \\ 0 & Z_{22}^{W_2} \end{pmatrix} \quad (2.5)$$

and

$$Z_{ij}^{W_3} = \begin{pmatrix} Z_{11}^{W_3} & Z_{12}^{W_3} & Z_{13}^{W_3} \\ 0 & Z_{22}^{W_3} & Z_{23}^{W_3} \\ 0 & 0 & Z_{33}^{W_3} \end{pmatrix}. \quad (2.6)$$

Again we avoid a clumsy index on the matrix elements by using a numerical map to the respective sets $\{W_2, \partial W_2\}$ and $\{W_3, \partial W_3, \partial \partial W_3\}$ respectively. Here the superscript indicates the level. Once these have been determined in a specific renormalization scheme then the anomalous dimension matrix is deduced from

$$\gamma_{ij}^{\mathcal{O}} = \mu \frac{d}{d\mu} \ln Z_{ij}^{\mathcal{O}} \quad (2.7)$$

with

$$\mu \frac{d}{d\mu} = \beta(a) \frac{\partial}{\partial a} + \alpha \gamma_\alpha(a, \alpha) \frac{\partial}{\partial \alpha} \quad (2.8)$$

where α is the gauge parameter of the canonical linear covariant gauge and $\alpha = 0$ corresponds to the Landau gauge. Although the operators we are considering are gauge invariant, in a mass dependent renormalization scheme, such as RI' or RI'/SMOM, the anomalous dimensions can depend on the gauge. This is why we have included the second term on the right side of (2.8). However, for the one loop computation here the leading term is scheme independent so that there is no gauge dependence at this order. In order to compare with the structure of our RI'/SMOM results later, we recall the three loop $\overline{\text{MS}}$ scheme anomalous dimension mixing matrices, [36], are

$$\begin{aligned} \gamma_{11}^{W_2}(a) &= \frac{8}{3} C_F a + \frac{1}{27} \left[376 C_A C_F - 112 C_F^2 - 128 C_F T_F N_f \right] a^2 \\ &+ \frac{1}{243} \left[(5184 \zeta(3) + 20920) C_A^2 C_F - (15552 \zeta(3) + 8528) C_A C_F^2 \right. \\ &\quad \left. - (10368 \zeta(3) + 6256) C_A C_F T_F N_f + (10368 \zeta(3) - 560) C_F^3 \right. \\ &\quad \left. + (10368 \zeta(3) - 6824) C_F^2 T_F N_f - 896 C_F T_F^2 N_f^2 \right] a^3 + O(a^4) \end{aligned}$$

$$\begin{aligned}
\gamma_{12}^{W_2}(a) &= -\frac{4}{3}C_F a + \frac{1}{27} \left[56C_F^2 - 188C_A C_F + 64C_F T_F N_f \right] a^2 \\
&\quad + \frac{1}{243} \left[(7776\zeta(3) + 4264) C_A C_F^2 - (2592\zeta(3) + 10460) C_A^2 C_F \right. \\
&\quad \quad \left. + (5184\zeta(3) + 3128) C_A C_F T_F N_f - (5184\zeta(3) - 280) C_F^3 \right. \\
&\quad \quad \left. - (5184\zeta(3) - 3412) C_F^2 T_F N_f + 448C_F T_F^2 N_f^2 \right] a^3 + O(a^4) \\
\gamma_{22}^{W_2}(a) &= O(a^4)
\end{aligned} \tag{2.9}$$

and

$$\begin{aligned}
\gamma_{11}^{W_3}(a) &= \frac{25}{6}C_F a + \frac{1}{432} \left[8560C_A C_F - 2035C_F^2 - 3320C_F T_F N_f \right] a^2 \\
&\quad + \frac{1}{15552} \left[(285120\zeta(3) + 1778866) C_A^2 C_F - (855360\zeta(3) + 311213) C_A C_F^2 \right. \\
&\quad \quad \left. - (1036800\zeta(3) + 497992) C_A C_F T_F N_f + (570240\zeta(3) - 244505) C_F^3 \right. \\
&\quad \quad \left. + (1036800\zeta(3) - 814508) C_F^2 T_F N_f - 82208C_F T_F^2 N_f^2 \right] a^3 + O(a^4) \\
\gamma_{12}^{W_3}(a) &= -\frac{3}{2}C_F a + \frac{1}{144} \left[81C_F^2 - 848C_A C_F + 424C_F T_F N_f \right] a^2 + O(a^3) \\
\gamma_{13}^{W_3}(a) &= -\frac{1}{2}C_F a + \frac{1}{144} \left[103C_F^2 - 388C_A C_F + 104C_F T_F N_f \right] a^2 + O(a^3) \\
\gamma_{22}^{W_3}(a) &= \frac{8}{3}C_F a + \frac{1}{27} \left[376C_A C_F - 112C_F^2 - 128C_F T_F N_f \right] a^2 \\
&\quad + \frac{1}{243} \left[(5184\zeta(3) + 20920) C_A^2 C_F - (15552\zeta(3) + 8528) C_A C_F^2 \right. \\
&\quad \quad \left. - (10368\zeta(3) + 6256) C_A C_F T_F N_f + (10368\zeta(3) - 560) C_F^3 \right. \\
&\quad \quad \left. + (10368\zeta(3) - 6824) C_F^2 T_F N_f - 896C_F T_F^2 N_f^2 \right] a^3 + O(a^4) \\
\gamma_{23}^{W_3}(a) &= -\frac{4}{3}C_F a + \frac{1}{27} \left[56C_F^2 - 188C_A C_F + 64C_F T_F N_f \right] a^2 \\
&\quad + \frac{1}{243} \left[(7776\zeta(3) + 4264) C_A C_F^2 - (2592\zeta(3) + 10460) C_A^2 C_F \right. \\
&\quad \quad \left. + (5184\zeta(3) + 3128) C_A C_F T_F N_f - (5184\zeta(3) - 280) C_F^3 \right. \\
&\quad \quad \left. - (5184\zeta(3) - 3412) C_F^2 T_F N_f + 448C_F T_F^2 N_f^2 \right] a^3 + O(a^4) \\
\gamma_{33}^{W_3}(a) &= O(a^4)
\end{aligned} \tag{2.10}$$

where $\zeta(z)$ is the Riemann zeta function, $a = g^2/(16\pi^2)$ and N_f is the number of massless quarks. The group Casimirs are defined by

$$T^a T^a = C_F, \quad \text{tr}(T^a T^b) = T_F \delta^{ab}, \quad f^{acd} f^{bcd} = C_A \delta^{ab} \tag{2.11}$$

where T^a are the Lie group generators with structure functions f^{abc} and $1 \leq a \leq N_A$ where N_A is the dimension of the adjoint representation.

We turn now to the set-up for the particular Green's function we are interested in which is $\langle \psi(p) \mathcal{O}_{\mu_1 \dots \mu_{n_i}}^i(-p - q) \bar{\psi}(q) \rangle$ and is illustrated in Figure 1. The independent external momenta we use are p and q and are the momenta flowing into the external quark legs. Thus there is a momentum of $p + q$ flowing out through the operator insertion whose location is indicated by the circle containing a cross. In order to determine the renormalization constants for the basic operators in the $\overline{\text{MS}}$ and RI' schemes one chooses $q = -p$. However, for the RI'/SMOM scheme the two momenta are left unconstrained. Instead to define the symmetric point of subtraction

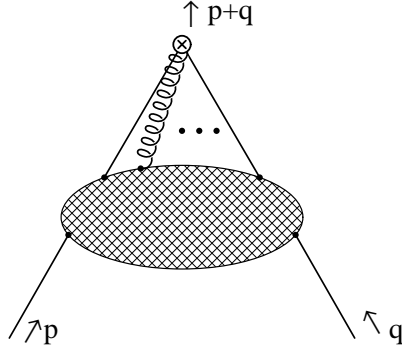


Figure 1: Graphical illustration of the Green's function, $\langle \psi(p) \mathcal{O}_{\mu_1 \dots \mu_{n_i}}^i(-p - q) \bar{\psi}(q) \rangle$, used to renormalize operators in the RI'/SMOM scheme.

for the renormalization the square of the momenta satisfy, [33, 34, 35],

$$p^2 = q^2 = (p + q)^2 = -\mu^2 \quad (2.12)$$

which imply

$$pq = \frac{1}{2}\mu^2 \quad (2.13)$$

where μ is the renormalization scale introduced to ensure the coupling constant is dimensionless in d -dimensions. Given this the Green's function is decomposed into a basis of independent Lorentz tensors, $\mathcal{P}_{(k)\mu_1 \dots \mu_{n_i}}^i(p, q)$, with associated amplitude, $\Sigma_{(k)}^{\mathcal{O}^i}(p, q)$, which is the value we will compute at the symmetric subtraction point,

$$\langle \psi(p) \mathcal{O}_{\mu_1 \dots \mu_{n_i}}^i(-p - q) \bar{\psi}(q) \rangle \Big|_{p^2 = q^2 = -\mu^2} = \sum_{k=1}^{n_i} \mathcal{P}_{(k)\mu_1 \dots \mu_{n_i}}^i(p, q) \Sigma_{(k)}^{\mathcal{O}^i}(p, q) . \quad (2.14)$$

Here the bracketed subscript k labels the projector and the superscript i is the operator level label, (2.1). The explicit tensors for each level are given in Appendix A together with the method which allows one to compute the amplitude itself via a projection onto the Green's function with free indices. The same tensor basis and projection is used for each level. The total number of projectors, n_i , is different for each level and recorded in Table 1. It is worth noting that the basis of projection tensors which we use for each level is not unique. They are constructed from the basic momentum vectors, γ -matrices and metric tensors available, in such a way that each final tensor has the same symmetry structure as its associated operator insertion, as well as being traceless in d -dimensions. Two final points concerning the projectors are worth emphasising. First, our choice of basis tensors, $\mathcal{P}_{(k)\mu_1 \dots \mu_{n_i}}^i(p, q)$, only has meaning strictly at the symmetric subtraction point. Away from this point there will be a bigger basis set of tensors since then we would have $p^2 \neq q^2$, $p^2 \neq (p + q)^2$ and $q^2 \neq (p + q)^2$ as is evident from the explicit forms given in Appendix A. Second, at the symmetric point the number of independent tensors in each case is clearly larger than that of the asymmetric forward subtraction point considered in the RI' scheme.

Given that there is more than one amplitude for each operator insertion, we have to be careful in defining the renormalization constant in the RI'/SMOM scheme. For the original scalar case, S , considered in [33] there is only one amplitude and therefore one does not need to be concerned about projection tensors. For all the cases we consider here the ultraviolet

i	V	T	W_2	W_3
n_i	5	6	8	11

Table 1. Number of projectors for each operator insertion.

divergence resides in a sub-set of the amplitudes which in fact contains at least one element. If, for the moment, we denote this representative projector by the label 0 then we define the renormalization constant for the operator \mathcal{O} , $Z_{\mathcal{O}}^{\text{RI}'/\text{SMOM}}$, by the condition

$$\lim_{\epsilon \rightarrow 0} \left[Z_{\psi}^{\text{RI}'} Z_{\mathcal{O}}^{\text{RI}'/\text{SMOM}} \Sigma_{(0)}^{\mathcal{O}}(p, q) \right] \Big|_{p^2 = q^2 = -\mu^2} = 1 \quad (2.15)$$

where $Z_{\psi}^{\text{RI}'}$ is the quark wave function renormalization constant in the RI' scheme which is given in [27, 28]. The reason why the value in the original RI' scheme is used has been discussed in [33, 34, 35]. In determining the final renormalization constant $Z_{\mathcal{O}}^{\text{RI}'/\text{SMOM}}$, we follow the procedure of [37] for automatic Feynman diagram computations. In other words we compute all diagrams in terms of their bare quantities which here are essentially the coupling constant and the gauge parameter. Then the renormalized parameters are introduced by rescaling with the already determined coupling constant and gauge parameter renormalization constants. Although the latter should be taken to be in the RI' scheme to the one loop order we are working any scheme effect will not show up until two loops. Whilst this is a standard procedure for introducing counterterms, the main issue here is that this rescaling from bare to renormalized quantities must also include the mixing of the operators. Therefore, in constructing our amplitudes, which are recorded in section three, the matrices (2.5) and (2.6) have been included. In practical terms this means that the renormalization constants are found by first fixing those in the last row of each matrix. Then those in the next row are determined and repeated until the ultimate row is found. This is similar to the method used in [36] to deduce (2.9) and (2.10). The basic reason for this bottom up approach is that the counterterms to be determined are intertwined due to the triangularity of the matrix and this is the systematic way to disentangle them.

Having concentrated on the general quantum field theoretic formalism that is used, we now comment on the practicalities of the calculation. We use standard tools for this. All the algebra is carried out with the symbolic manipulation language FORM, [38]. The three one loop Feynman diagrams are generated in electronic form by the QGRAF package, [39], with the output converted into FORM input notation. This procedure appends indices and labels to all the fields. Various FORM modules were then used to insert the basic Feynman rules for the propagators and vertices before those of the particular operator of interest. The n_i amplitudes were then projected out by the theory given in Appendix A for successive Green's functions. The final part is to break up the resulting scalar integral into a base set of master one loop integrals. This may have required integration by parts but for the most part the resulting integrals are one loop with only two propagators. These bubbles are simple to determine. The remaining integral is

$$\int \frac{d^d k}{(2\pi)^d} \frac{1}{k^2 (k-p)^2 (k+q)^2} \Big|_{p^2 = q^2 = -\mu^2} = \frac{9s_2}{\mu^2} + O(\epsilon) \quad (2.16)$$

where $s_2 = (2\sqrt{3}/9)\text{Cl}_2(2\pi/3)$ and $\text{Cl}_2(x)$ is the Clausen function which was evaluated in [40]. We use dimensional regularization in $d = 4 - 2\epsilon$ dimensions. Given these ingredients we have been able to determine all the one loop amplitudes for the set of operators (2.1) where we have repeated the calculation for S as an elementary check on our programmes. We correctly reproduced the one loop expressions given in [33, 34, 35].

3 Results.

Having concentrated on describing the background to the problem and the methodology of the computations, we turn to the mundane task of recording the explicit results. We do this successively for the vector, tensor and the two moments of the Wilson operators. First, for the vector case we have,

$$\begin{aligned}\Sigma_{(1)}^V(p, q) &= -1 + O(a^2), \\ \Sigma_{(2)}^V(p, q) &= \Sigma_{(5)}^V(p, q) = - \left[6s_2 - \frac{8}{3} - 6s_2\alpha + \frac{4}{3}\alpha \right] a + O(a^2), \\ \Sigma_{(3)}^V(p, q) &= \Sigma_{(4)}^V(p, q) = \left[\frac{4}{3} - \frac{2}{3}\alpha + 6s_2\alpha \right] a + O(a^2).\end{aligned}\quad (3.1)$$

To make contact with other work in this area, [33], we note the relations

$$C_0(1) = 9s_2 = \frac{2}{3}\psi' \left(\frac{1}{3} \right) - \left(\frac{2\pi}{3} \right)^2 \quad (3.2)$$

where $\psi(z)$ is the derivative of the logarithm of the Euler Γ -function and $C_0(\omega)$ was the function used in [33] to interpolate between the symmetric and exceptional momenta scheme choices. As this particular Green's function is symmetric under swapping the two independent momenta, then two pairs of the amplitudes are equivalent. Also, since the operator is a physical operator there is no divergence in the operator renormalization constant. However, there is a finite part given the nature of the renormalization scheme. We have

$$Z^V = 1 + C_F [2 - 3s_2 - \alpha + 6s_2\alpha] a + O(a^2). \quad (3.3)$$

For the tensor case there is a degree of simplicity with the amplitudes which is on a par with what was observed in the RI' scheme renormalization of [28]. However, in this case there is a one loop contribution to projection tensor number 6 of the basis and we note that this tensor has no γ -matrix part since it is proportional to the unit matrix of spinor space. This particular tensor is absent when either the two independent momenta are equal or when one is zero. In the latter case this would correspond to the momentum configuration where the external momentum flowing into a quark leg is nullified leaving the momentum flowing out through the operator itself. This is not the same configuration as was used in the RI' computations of [28]. In other words in considering the Green's function with two independent momenta one has to be aware of tensor structures which do not necessarily have the same spinor or γ -matrix structure as the original operator itself even in the case when there is no quark masses present. So the amplitudes are

$$\begin{aligned}\Sigma_{(1)}^T(p, q) &= -1 + O(a^2), \\ \Sigma_{(2)}^T(p, q) &= \Sigma_{(3)}^T(p, q) = \Sigma_{(4)}^T(p, q) = \Sigma_{(5)}^T(p, q) = O(a^2), \\ \Sigma_{(6)}^T(p, q) &= [9s_2 + 3s_2\alpha] a + O(a^2)\end{aligned}\quad (3.4)$$

and the associated renormalization constant is

$$Z^T = 1 + C_F \left[\frac{1}{\epsilon} + \frac{4}{3} - \frac{9}{2}s_2 - \frac{1}{3}\alpha + \frac{9}{2}s_2\alpha \right] a + O(a^2). \quad (3.5)$$

The divergent part agrees with the $\overline{\text{MS}}$ divergence as it ought to since the one loop anomalous dimensions are scheme independent. This, of course, will be the situation with the other renormalization constants irrespective of whether there is mixing or not. Moreover, the finite part of (3.5) is in total agreement with [33].

The situation for both moments of the flavour non-singlet twist-2 Wilson operators is more involved due to the operator mixing issue. First, for $n = 2$ we find the amplitudes are

$$\begin{aligned}
\Sigma_{(1)}^{W_2}(p, q) &= O(a^2) , \quad \Sigma_{(2)}^{W_2}(p, q) = -1 + O(a^2) , \\
\Sigma_{(3)}^{W_2}(p, q) &= \left[\frac{4}{3}s_2 - \frac{8}{9}\alpha + \frac{16}{27} + 4s_2\alpha \right] a + O(a^2) , \\
\Sigma_{(4)}^{W_2}(p, q) &= - \left[\frac{16}{3}s_2 - \frac{71}{27} - 8s_2\alpha + \frac{16}{9}\alpha \right] a + O(a^2) , \\
\Sigma_{(5)}^{W_2}(p, q) &= - \left[\frac{20}{3}s_2 - \frac{100}{27} - 16s_2\alpha + \frac{26}{9}\alpha \right] a + O(a^2) , \\
\Sigma_{(6)}^{W_2}(p, q) &= \left[\frac{20}{3}s_2 - \frac{28}{27} - 4s_2\alpha + \frac{14}{9}\alpha \right] a + O(a^2) , \\
\Sigma_{(7)}^{W_2}(p, q) &= - \left[\frac{2}{3}s_2 - \frac{37}{27} - 4s_2\alpha + \frac{2}{9}\alpha \right] a + O(a^2) , \\
\Sigma_{(8)}^{W_2}(p, q) &= - \left[\frac{40}{3}s_2 - \frac{128}{27} - 8s_2\alpha + \frac{16}{9}\alpha \right] a + O(a^2) , \\
\Sigma_{(1)}^{\partial W_2}(p, q) &= \Sigma_{(2)}^{\partial W_2}(p, q) = -1 + O(a^2) , \\
\Sigma_{(3)}^{\partial W_2}(p, q) &= \Sigma_{(8)}^{\partial W_2}(p, q) = - \left[12s_2 - \frac{16}{3} - 12s_2\alpha + \frac{8}{3}\alpha \right] a + O(a^2) , \\
\Sigma_{(4)}^{\partial W_2}(p, q) &= \Sigma_{(7)}^{\partial W_2}(p, q) = - [6s_2 - 4 - 12s_2\alpha + 2\alpha] a + O(a^2) , \\
\Sigma_{(5)}^{\partial W_2}(p, q) &= \Sigma_{(6)}^{\partial W_2}(p, q) = - \left[\frac{4}{3}\alpha - \frac{8}{3} - 12s_2\alpha \right] a + O(a^2)
\end{aligned} \tag{3.6}$$

where the operator superscript label here corresponds to the row of the matrix with that operator on the diagonal. Unlike the previous two cases there is now no symmetry for the Green's function itself when the original operator is inserted. This is because the covariant derivative in the operator only acts on the quark and not the anti-quark. So swapping the external momenta in the Green's function is not a symmetric operation. By contrast for the associated total derivative operator this symmetry is still valid which is why there are equivalences between three pairs of amplitudes. Moreover, the actual expressions for the tensors labelled 3 and 5 are proportional to those labelled 2 and 3 of the vector case. This is not unexpected because the total derivative operator associated with this moment is effectively the vector current in disguise at the higher level. That the expressions are not precisely the same is due to the fact that one has an extra Lorentz index present at this level so that the projection coefficient into the basis will not have a completely parallel value. Although there is no unique basis for the projection tensors this agreement at one loop is a check on our calculational setup particularly since with another choice of tensors this proportionality could have been hidden. For the renormalization constants the relation between the divergences has already been noted at three loops in the $\overline{\text{MS}}$ scheme in [36]. However, now that there are finite parts in the RI'/SMOM scheme we note that there is an interesting relation at one loop. Since

$$\begin{aligned}
Z_{11}^{W_2} &= 1 + C_F \left[\frac{8}{3\epsilon} + \frac{17}{3} - 7s_2 - \frac{1}{3}\alpha + 6s_2\alpha \right] a + O(a^2) , \\
Z_{12}^{W_2} &= C_F \left[-\frac{4}{3\epsilon} - \frac{11}{6} + 2s_2 - \frac{1}{3}\alpha \right] a + O(a^2) , \\
Z_{22}^{W_2} &= 1 + C_F [2 - 3s_2 - \alpha + 6s_2\alpha] a + O(a^2)
\end{aligned} \tag{3.7}$$

then it is straightforward to see

$$Z_{11}^{W_2} = Z_{22}^{W_2} - 2Z_{12}^{W_2} + O(a^2) . \tag{3.8}$$

Whether this is just a peculiarity for W_2 which does not extend beyond one loop or representative of a deeper origin, cannot be ascertained until a two loop computation is available. Though the amplitudes satisfy a similar relation

$$\Sigma_{(3)}^{\partial W_2}(p, q) - 2\Sigma_{(4)}^{\partial W_2}(p, q) + \Sigma_{(5)}^{\partial W_2}(p, q) = O(a^2) \quad (3.9)$$

as well.

For the next moment the situation is of course more substantial since there are eleven different basis tensors and three operators which mix. First, we record the amplitudes to one loop are

$$\begin{aligned} \Sigma_{(1)}^{W_3}(p, q) &= O(a^2), \quad \Sigma_{(2)}^{W_3}(p, q) = O(a^2), \\ \Sigma_{(3)}^{W_3}(p, q) &= -\frac{1}{3} + O(a^2), \quad \Sigma_{(4)}^{W_3}(p, q) = -\left[2s_2 - \frac{7}{9} - \frac{26}{9}s_2\alpha + \frac{58}{81}\alpha\right]a + O(a^2), \\ \Sigma_{(5)}^{W_3}(p, q) &= -\left[\frac{8}{9}s_2 - \frac{89}{162} - \frac{22}{9}s_2\alpha + \frac{47}{81}\alpha\right]a + O(a^2), \\ \Sigma_{(6)}^{W_3}(p, q) &= -\left[\frac{32}{9}s_2 - \frac{221}{162} - \frac{44}{9}s_2\alpha + \frac{94}{81}\alpha\right]a + O(a^2), \\ \Sigma_{(7)}^{W_3}(p, q) &= -\left[\frac{20}{3}s_2 - \frac{137}{54} - \frac{100}{9}s_2\alpha + \frac{194}{81}\alpha\right]a + O(a^2), \\ \Sigma_{(8)}^{W_3}(p, q) &= -\left[\frac{14}{81}\alpha - \frac{1}{6} - \frac{10}{9}s_2\alpha\right]a + O(a^2), \\ \Sigma_{(9)}^{W_3}(p, q) &= \left[\frac{2}{9}s_2 + \frac{25}{162} + \frac{2}{9}s_2\alpha + \frac{8}{81}\alpha\right]a + O(a^2), \\ \Sigma_{(10)}^{W_3}(p, q) &= -\left[\frac{16}{9}s_2 - \frac{133}{162} - \frac{16}{9}s_2\alpha + \frac{17}{81}\alpha\right]a + O(a^2), \\ \Sigma_{(11)}^{W_3}(p, q) &= -\left[\frac{28}{3}s_2 - \frac{77}{27} - \frac{44}{9}s_2\alpha + \frac{94}{81}\alpha\right]a + O(a^2), \\ \Sigma_{(1)}^{\partial W_3}(p, q) &= O(a^2), \quad \Sigma_{(2)}^{\partial W_3}(p, q) = -\frac{1}{6} + O(a^2), \\ \Sigma_{(3)}^{\partial W_3}(p, q) &= -\frac{1}{3} + O(a^2), \quad \Sigma_{(4)}^{\partial W_3}(p, q) = -\left[\frac{4}{9}\alpha - \frac{2}{3}s_2 - \frac{8}{27} - 2s_2\alpha\right]a + O(a^2), \\ \Sigma_{(5)}^{\partial W_3}(p, q) &= -\left[\frac{14}{9}s_2 - \frac{79}{81} - \frac{10}{3}s_2\alpha + \frac{20}{27}\alpha\right]a + O(a^2), \\ \Sigma_{(6)}^{\partial W_3}(p, q) &= -\left[\frac{26}{9}s_2 - \frac{121}{81} - \frac{16}{3}s_2\alpha + \frac{29}{27}\alpha\right]a + O(a^2), \\ \Sigma_{(7)}^{\partial W_3}(p, q) &= -\left[\frac{10}{3}s_2 - \frac{50}{27} - 8s_2\alpha + \frac{13}{9}\alpha\right]a + O(a^2), \\ \Sigma_{(8)}^{\partial W_3}(p, q) &= \left[\frac{10}{3}s_2 - \frac{14}{27} - 2s_2\alpha + \frac{7}{9}\alpha\right]a + O(a^2), \\ \Sigma_{(9)}^{\partial W_3}(p, q) &= \left[\frac{8}{9}s_2 + \frac{23}{81} + \frac{2}{3}s_2\alpha + \frac{5}{27}\alpha\right]a + O(a^2), \\ \Sigma_{(10)}^{\partial W_3}(p, q) &= -\left[\frac{22}{9}s_2 - \frac{101}{81} - \frac{8}{3}s_2\alpha + \frac{10}{27}\alpha\right]a + O(a^2), \\ \Sigma_{(11)}^{\partial W_3}(p, q) &= -\left[\frac{20}{3}s_2 - \frac{64}{27} - 4s_2\alpha + \frac{8}{9}\alpha\right]a + O(a^2), \\ \Sigma_{(1)}^{\partial\partial W_3}(p, q) &= \Sigma_{(2)}^{\partial\partial W_3}(p, q) = \Sigma_{(3)}^{\partial\partial W_3}(p, q) = -\frac{1}{3} + O(a^2), \\ \Sigma_{(4)}^{\partial\partial W_3}(p, q) &= \Sigma_{(11)}^{\partial\partial W_3}(p, q) = -\left[6s_2 - \frac{8}{3} - 6s_2\alpha + \frac{4}{3}\alpha\right]a + O(a^2), \end{aligned}$$

$$\begin{aligned}
\Sigma_{(5)}^{\partial\partial W_3}(p, q) &= \Sigma_{(10)}^{\partial\partial W_3}(p, q) = - \left[4s_2 - \frac{20}{9} - 6s_2\alpha + \frac{10}{9}\alpha \right] a + O(a^2), \\
\Sigma_{(6)}^{\partial\partial W_3}(p, q) &= \Sigma_{(9)}^{\partial\partial W_3}(p, q) = - \left[2s_2 - \frac{16}{9} - 6s_2\alpha + \frac{8}{9}\alpha \right] a + O(a^2), \\
\Sigma_{(7)}^{\partial\partial W_3}(p, q) &= \Sigma_{(8)}^{\partial\partial W_3}(p, q) = - \left[\frac{2}{3}\alpha - \frac{4}{3} - 6s_2\alpha \right] a + O(a^2).
\end{aligned} \tag{3.10}$$

As with the lower moment there are similar relations to one loop. First, there is an obvious parallel with the vector and total derivative operator for $n = 2$ with the double total derivative of the third moment which was noted in [36]. In addition there are cross connections with the central row of the mixing matrix. Specifically, the amplitudes labelled 6 and 8 of W_2 are proportional to 8 and 11 of ∂W_3 respectively for the same reasons as before. Further, there is another apparent relation within the level since

$$\Sigma_{(5)}^{\partial\partial W_3}(p, q) - 2\Sigma_{(6)}^{\partial\partial W_3}(p, q) + \Sigma_{(7)}^{\partial\partial W_3}(p, q) = O(a^2) \tag{3.11}$$

in addition to the reflection of the one already noted for moment $n = 2$. Indeed the associated renormalization constants also satisfy a similar underlying relation as is evident by studying the full set which is

$$\begin{aligned}
Z_{11}^{W_3} &= 1 + C_F \left[\frac{25}{6\epsilon} + \frac{307}{36} - 9s_2 - \frac{4}{9}\alpha + 8s_2\alpha \right] a + O(a^2), \\
Z_{12}^{W_3} &= C_F \left[-\frac{3}{2\epsilon} - \frac{103}{36} + 2s_2 + \frac{1}{9}\alpha - 2s_2\alpha \right] a + O(a^2), \\
Z_{13}^{W_3} &= C_F \left[-\frac{1}{2\epsilon} - \frac{1}{36} - s_2 - \frac{11}{18}\alpha + 2s_2\alpha \right] a + O(a^2), \\
Z_{22}^{W_3} &= 1 + C_F \left[\frac{8}{3\epsilon} + \frac{17}{3} - 7s_2 - \frac{1}{3}\alpha + 6s_2\alpha \right] a + O(a^2), \\
Z_{23}^{W_3} &= C_F \left[-\frac{4}{3\epsilon} - \frac{11}{6} + 2s_2 - \frac{1}{3}\alpha \right] a + O(a^2), \\
Z_{33}^{W_3} &= 1 + C_F [2 - 3s_2 - \alpha + 6s_2\alpha] a + O(a^2).
\end{aligned} \tag{3.12}$$

Again these relations provide useful internal checks on both the integration routines and the construction of the projection matrix and its implementation in FORM. As an aside we note that in highlighting these relations of the amplitudes we have concentrated on those which are gauge independent. There appears to be other relations which are only valid to one loop in the Landau gauge and since the case for regarding these as significant is diminished because of the apparent gauge dependence we do not draw attention to them.

As our computations have been at one loop the conversion functions that are used to convert from the $\overline{\text{MS}}$ scheme to the RI'/SMOM scheme are in effect the finite parts of the renormalization constants themselves. See, for example, [41]. Therefore, in order to appreciate the magnitude of the one loop contribution it is a straightforward exercise to evaluate the finite parts numerically. It turns out that the correction increases in value with the operator moment, in parallel, for example, with the numerical value of the one loop anomalous dimension coefficient. If we take the Landau gauge case and compare the finite parts, the vector and moments $n = 2$ and 3 are respectively, 1.2187, 3.8436 and 6.1839 where we use the (11) element for the latter two or equivalently the diagonal of the W_3 matrix. This is with ignoring the common colour factor, C_F , and coupling constant, a . Therefore, for higher moments it would seem that one would require higher loop corrections in order to have a more reliable convergence of the perturbative series for the conversion functions. Comparing with the RI' scheme results of [28, 29, 30] the respective numbers are 0, 3.4444 and 5.9444. Unlike the situation with the mass operator the RI'/SMOM

scheme corrections for W_2 and W_3 are slightly larger. Though in some sense this is not a fair comparison because of the mixing. The RI' scheme is based on a specific momentum routing in the Green's function which is blind to the off-diagonal matrix element of the renormalization constant matrix. In the case of the vector operator the finite part of the RI' renormalization depends only on the gauge parameter at one loop. So one would require the next loop order in order to have a reasonable comparison and indication of the overall convergence. This last remark equally applies to the W_2 and W_3 cases.

4 Discussion.

We have determined the renormalization constants at one loop for the twist-2 flavour non-singlet operators with moments $n = 2$ and 3 in the RI'/SMOM scheme and have taken account of operator mixing. In the Landau gauge the correction increases in value with the operator moment. So it would appear that the series for the conversion function will converge slower at high moment. Of course, a one loop computation is not sufficient to make a definitive statement since the higher loop corrections may produce an improvement. Indeed with the recent work of [34, 35] for bilinear quark currents it would seem that an extension of the Wilson operator calculation we have performed here could be produced in the foreseeable future. Equally it would be useful to see how the lattice measurements in this symmetric scheme for the deep inelastic scattering operators compares with the same analysis in the earlier RI' scheme. Though it may be the case that not all the various tensor projections would give a clear accurate numerical signal. Finally, whilst the RI'/SMOM scheme is designed in order to circumvent infrared problems, one is still restricted to the Landau gauge due to the fact that the Green's function of Figure 1 is a gauge dependent quantity. Whilst this is not a problem for the high energy régime, it may be the case that in the infrared there are additional complications with Gribov copies and hence the definitive measurement of operator matrix elements.

Acknowledgement. The author thanks Dr. P.E.L. Rakow and Prof. C.T.C. Sachrajda for useful discussions and especially the former for a careful reading of the manuscript.

A Projectors.

In this appendix we record in succession the basis of projection tensors we have used in each of the various cases. These were denoted earlier by the general notation $\mathcal{P}_{(k)\mu_1\dots\mu_{n_i}}^i(p, q)$. The matrix, \mathcal{M}_{kl}^i , in the second part of each subsection contains the coefficients associated with each basis projection tensor, which allows one to project out the amplitudes $\Sigma_{(k)}^{\mathcal{O}^i}(p, q)$. It is constructed by first determining the matrix

$$\mathcal{N}_{kl}^i = \mathcal{P}_{(k)\mu_1\dots\mu_{n_i}}^i(p, q) \mathcal{P}_{(l)}^{\mu_1\dots\mu_{n_i}}(p, q) \Big|_{p^2=q^2=-\mu^2} \quad (\text{A.1})$$

where there is no summation over the label i and k and l index the projection tensors. Given that the elements are contractions of Lorentz tensors in d -dimensions then the elements of \mathcal{N}_{kl}^i are polynomials in d . Finally, \mathcal{M}_{kl}^i is the inverse of \mathcal{N}_{kl}^i and

$$\Sigma_{(k)}^{\mathcal{O}^i}(p, q) = \mathcal{M}_{kl}^i \mathcal{P}_{(l)}^{\mu_1\dots\mu_{n_i}}(p, q) \left(\left\langle \psi(p) \mathcal{O}_{\mu_1\dots\mu_{n_i}}^i(-p-q) \bar{\psi}(q) \right\rangle \right) \Big|_{p^2=q^2=-\mu^2} \quad (\text{A.2})$$

where again there is no summation over the level label i .

A.1 Vector.

$$\begin{aligned}\mathcal{P}_{(1)\mu}^V(p, q) &= \gamma_\mu, \quad \mathcal{P}_{(2)\mu}^V(p, q) = \frac{p^\mu \not{p}}{\mu^2}, \quad \mathcal{P}_{(3)\mu}^V(p, q) = \frac{p_\mu \not{q}}{\mu^2}, \\ \mathcal{P}_{(4)\mu}^V(p, q) &= \frac{q_\mu \not{p}}{\mu^2}, \quad \mathcal{P}_{(5)\mu}^V(p, q) = \frac{q_\mu \not{q}}{\mu^2},\end{aligned}\quad (\text{A.3})$$

$$\mathcal{M}^V = \frac{1}{36(d-2)} \begin{pmatrix} 9 & 12 & 6 & 6 & 12 \\ 12 & 16(d-1) & 8(d-1) & 8(d-1) & 4(d+2) \\ 6 & 8(d-1) & 4(4d-7) & 4(d-1) & 8(d-1) \\ 6 & 8(d-1) & 4(d-1) & 4(4d-7) & 8(d-1) \\ 12 & 4(d+2) & 8(d-1) & 8(d-1) & 16(d-1) \end{pmatrix}. \quad (\text{A.4})$$

A.2 Tensor.

$$\begin{aligned}\mathcal{P}_{(1)\mu\nu}^T(p, q) &= \sigma_{\mu\nu}, \quad \mathcal{P}_{(2)\mu\nu}^T(p, q) = \frac{1}{\mu^2} [\gamma_\mu \not{p} p_\nu - \gamma_\nu \not{p} p_\mu], \\ \mathcal{P}_{(3)\mu\nu}^T(p, q) &= \frac{1}{\mu^2} [\gamma_\mu \not{p} q_\nu - \gamma_\nu \not{p} q_\mu], \quad \mathcal{P}_{(4)\mu\nu}^T(p, q) = \frac{1}{\mu^2} [\gamma_\mu \not{q} p_\nu - \gamma_\nu \not{q} p_\mu], \\ \mathcal{P}_{(5)\mu\nu}^T(p, q) &= \frac{1}{\mu^2} [\gamma_\mu \not{q} q_\nu - \gamma_\nu \not{q} q_\mu], \quad \mathcal{P}_{(6)\mu\nu}^T(p, q) = \frac{1}{\mu^2} [p_\mu q_\nu - q_\mu p_\nu],\end{aligned}\quad (\text{A.5})$$

$$\mathcal{M}^T = \frac{1}{36(d-2)^2} \begin{pmatrix} -\frac{9d}{d-1} & -12 & -6 & -6 & -12 & 0 \\ -12 & -8(d-1) & -4(d-1) & -4(d-1) & -2(d+2) & 0 \\ -6 & -4(d-1) & -2(4d-7) & -2(d-1) & -4(d-1) & 6(d-2) \\ -6 & -4(d-1) & -2(d-1) & -2(4d-7) & -4(d-1) & -6(d-2) \\ -12 & -2(d+2) & -4(d-1) & -4(d-1) & -8(d-1) & 0 \\ 0 & 0 & 6(d-2) & -6(d-2) & 0 & 6(d-2)(d-4) \end{pmatrix}. \quad (\text{A.6})$$

A.3 Wilson 2.

$$\begin{aligned}\mathcal{P}_{(1)\mu\nu}^{W_2}(p, q) &= \gamma_\mu p_\nu + \gamma_\nu p_\mu - \frac{2}{d} \not{p} \eta_{\mu\nu}, \quad \mathcal{P}_{(2)\mu\nu}^{W_2}(p, q) = \gamma_\mu q_\nu + \gamma_\nu q_\mu - \frac{2}{d} \not{q} \eta_{\mu\nu}, \\ \mathcal{P}_{(3)\mu\nu}^{W_2}(p, q) &= \not{p} \left[\frac{1}{\mu^2} p_\mu p_\nu + \frac{1}{d} \not{p} \eta_{\mu\nu} \right], \quad \mathcal{P}_{(4)\mu\nu}^{W_2}(p, q) = \not{p} \left[\frac{1}{\mu^2} p_\mu q_\nu + \frac{1}{\mu^2} q_\mu p_\nu - \frac{1}{d} \eta_{\mu\nu} \right], \\ \mathcal{P}_{(5)\mu\nu}^{W_2}(p, q) &= \not{p} \left[\frac{1}{\mu^2} q_\mu q_\nu + \frac{1}{d} \not{p} \eta_{\mu\nu} \right], \quad \mathcal{P}_{(6)\mu\nu}^{W_2}(p, q) = \not{q} \left[\frac{1}{\mu^2} p_\mu p_\nu + \frac{1}{d} \not{p} \eta_{\mu\nu} \right], \\ \mathcal{P}_{(7)\mu\nu}^{W_2}(p, q) &= \not{q} \left[\frac{1}{\mu^2} p_\mu q_\nu + \frac{1}{\mu^2} q_\mu p_\nu - \frac{1}{d} \eta_{\mu\nu} \right], \quad \mathcal{P}_{(8)\mu\nu}^{W_2}(p, q) = \not{q} \left[\frac{1}{\mu^2} q_\mu q_\nu + \frac{1}{d} \not{p} \eta_{\mu\nu} \right].\end{aligned}\quad (\text{A.7})$$

To save space for the projection matrix in this case, we have partitioned the 8×8 matrix into four sub-matrices. We have

$$\begin{aligned}\mathcal{M}^{W_2} &= -\frac{1}{108(d-2)} \begin{pmatrix} \mathcal{M}_{11}^{W_2} & \mathcal{M}_{12}^{W_2} \\ \mathcal{M}_{21}^{W_2} & \mathcal{M}_{22}^{W_2} \end{pmatrix}, \\ \mathcal{M}_{11}^{W_2} &= \begin{pmatrix} 18 & 9 & 48 & 24 \\ 9 & 18 & 24 & 30 \\ 48 & 24 & 64(d+1) & 32(d+2) \\ 24 & 30 & 32(d+1) & 8(5d-1) \end{pmatrix},\end{aligned}$$

$$\begin{aligned}
\mathcal{M}_{12}^{W_2} &= \begin{pmatrix} 12 & 24 & 30 & 24 \\ 24 & 12 & 24 & 48 \\ 16(d+4) & 32(d+1) & 16(d+4) & 8(d+10) \\ 8(4d+1) & 16(d+1) & 20(d+1) & 16(d+4) \end{pmatrix}, \\
\mathcal{M}_{21}^{W_2} &= \begin{pmatrix} 12 & 24 & 16(d+4) & 8(4d+1) \\ 24 & 12 & 32(d+1) & 8(d+4) \\ 30 & 24 & 16(d+4) & 20(d+1) \\ 24 & 48 & 8(d+10) & 16(d+4) \end{pmatrix}, \\
\mathcal{M}_{22}^{W_2} &= \begin{pmatrix} 32(2d-1) & 8(d+4) & 16(d+1) & 32(d+1) \\ 8(d+4) & 32(2d-1) & 8(4d+1) & 16(d+4) \\ 16(d+1) & 8(4d+1) & 8(5d-1) & 32(d+1) \\ 32(d+1) & 16(d+4) & 32(d+1) & 64(d+1) \end{pmatrix}. \tag{A.8}
\end{aligned}$$

A.4 Wilson 3.

$$\begin{aligned}
\mathcal{P}_{(1)\mu\nu}^{W_3}(p, q) &= \frac{1}{\mu^2} [\gamma_\mu p_\nu p_\sigma + \gamma_\nu p_\sigma p_\mu + \gamma_\sigma p_\mu p_\nu] + \frac{1}{[d+2]} [\gamma_\mu \eta_{\nu\sigma} + \gamma_\nu \eta_{\sigma\mu} + \gamma_\sigma \eta_{\mu\nu}] \\
&\quad - \frac{2\phi}{[d+2]\mu^2} [\eta_{\mu\nu} p_\sigma + \eta_{\nu\sigma} p_\mu + \eta_{\sigma\mu} p_\nu], \\
\mathcal{P}_{(2)\mu\nu}^{W_3}(p, q) &= \frac{1}{\mu^2} [\gamma_\mu p_\nu q_\sigma + \gamma_\nu p_\sigma q_\mu + \gamma_\sigma p_\mu q_\nu + \gamma_\mu q_\nu p_\sigma + \gamma_\nu q_\sigma p_\mu + \gamma_\sigma q_\mu p_\nu] \\
&\quad - \frac{1}{[d+2]} [\gamma_\mu \eta_{\nu\sigma} + \gamma_\nu \eta_{\sigma\mu} + \gamma_\sigma \eta_{\mu\nu}] - \frac{2\phi}{[d+2]\mu^2} [\eta_{\mu\nu} q_\sigma + \eta_{\nu\sigma} q_\mu + \eta_{\sigma\mu} q_\nu] \\
&\quad - \frac{2\phi}{[d+2]\mu^2} [\eta_{\mu\nu} p_\sigma + \eta_{\nu\sigma} p_\mu + \eta_{\sigma\mu} p_\nu], \\
\mathcal{P}_{(3)\mu\nu}^{W_3}(p, q) &= \frac{1}{\mu^2} [\gamma_\mu q_\nu q_\sigma + \gamma_\nu q_\sigma q_\mu + \gamma_\sigma q_\mu q_\nu] + \frac{1}{[d+2]} [\gamma_\mu \eta_{\nu\sigma} + \gamma_\nu \eta_{\sigma\mu} + \gamma_\sigma \eta_{\mu\nu}] \\
&\quad - \frac{2\phi}{[d+2]\mu^2} [\eta_{\mu\nu} q_\sigma + \eta_{\nu\sigma} q_\mu + \eta_{\sigma\mu} q_\nu], \\
\mathcal{P}_{(4)\mu\nu}^{W_3}(p, q) &= \frac{\phi}{\mu^4} p_\mu p_\nu p_\sigma + \frac{\phi}{[d+2]\mu^2} [\eta_{\mu\nu} p_\sigma + \eta_{\nu\sigma} p_\mu + \eta_{\sigma\mu} p_\nu], \\
\mathcal{P}_{(5)\mu\nu}^{W_3}(p, q) &= \frac{\phi}{\mu^4} [p_\mu p_\nu q_\sigma + p_\mu q_\nu p_\sigma + q_\mu p_\nu p_\sigma] \\
&\quad - \frac{\phi}{[d+2]\mu^2} [\eta_{\mu\nu} p_\sigma - \eta_{\mu\nu} q_\sigma + \eta_{\nu\sigma} p_\mu - \eta_{\nu\sigma} q_\mu + \eta_{\sigma\mu} p_\nu - \eta_{\sigma\mu} q_\nu], \\
\mathcal{P}_{(6)\mu\nu}^{W_3}(p, q) &= \frac{\phi}{\mu^4} [p_\mu q_\nu q_\sigma + q_\mu p_\nu q_\sigma + q_\mu q_\nu p_\sigma] \\
&\quad + \frac{\phi}{[d+2]\mu^2} [\eta_{\mu\nu} p_\sigma - \eta_{\mu\nu} q_\sigma + \eta_{\nu\sigma} p_\mu - \eta_{\nu\sigma} q_\mu + \eta_{\sigma\mu} p_\nu - \eta_{\sigma\mu} q_\nu], \\
\mathcal{P}_{(7)\mu\nu}^{W_3}(p, q) &= \frac{\phi}{\mu^4} q_\mu q_\nu q_\sigma + \frac{\phi}{[d+2]\mu^2} [\eta_{\mu\nu} q_\sigma + \eta_{\nu\sigma} q_\mu + \eta_{\sigma\mu} q_\nu], \\
\mathcal{P}_{(8)\mu\nu}^{W_3}(p, q) &= \frac{\phi}{\mu^4} p_\mu p_\nu p_\sigma + \frac{\phi}{[d+2]\mu^2} [\eta_{\mu\nu} p_\sigma + \eta_{\nu\sigma} p_\mu + \eta_{\sigma\mu} p_\nu], \\
\mathcal{P}_{(9)\mu\nu}^{W_3}(p, q) &= \frac{\phi}{\mu^4} [p_\mu p_\nu q_\sigma + p_\mu q_\nu p_\sigma + q_\mu p_\nu p_\sigma] \\
&\quad - \frac{\phi}{[d+2]\mu^2} [\eta_{\mu\nu} p_\sigma - \eta_{\mu\nu} q_\sigma + \eta_{\nu\sigma} p_\mu - \eta_{\nu\sigma} q_\mu + \eta_{\sigma\mu} p_\nu - \eta_{\sigma\mu} q_\nu],
\end{aligned}$$

$$\begin{aligned}
\mathcal{P}_{(10)\mu\nu}^{W_3}(p, q) &= \frac{q}{\mu^4} [p_\mu q_\nu q_\sigma + q_\mu p_\nu q_\sigma + q_\mu q_\nu p_\sigma] \\
&\quad + \frac{q}{[d+2]\mu^2} [\eta_{\mu\nu} p_\sigma - \eta_{\mu\nu} q_\sigma + \eta_{\nu\sigma} p_\mu - \eta_{\nu\sigma} q_\mu + \eta_{\sigma\mu} p_\nu - \eta_{\sigma\mu} q_\nu] , \\
\mathcal{P}_{(11)\mu\nu}^{W_3}(p, q) &= \frac{q}{\mu^4} q_\mu q_\nu q_\sigma + \frac{q}{[d+2]\mu^2} [\eta_{\mu\nu} q_\sigma + \eta_{\nu\sigma} q_\mu + \eta_{\sigma\mu} q_\nu] .
\end{aligned} \tag{A.9}$$

Similar to the previous case we have subdivided the 11×11 matrix here into nine submatrices in order to ease the presentation. We have

$$\begin{aligned}
\mathcal{M}^{W_3} &= \frac{1}{2106d(d-2)} \begin{pmatrix} \mathcal{M}_{11}^{W_3} & \mathcal{M}_{12}^{W_3} & \mathcal{M}_{13}^{W_3} \\ \mathcal{M}_{21}^{W_3} & \mathcal{M}_{22}^{W_3} & \mathcal{M}_{23}^{W_3} \\ \mathcal{M}_{31}^{W_3} & \mathcal{M}_{32}^{W_3} & \mathcal{M}_{33}^{W_3} \end{pmatrix} , \\
\mathcal{M}_{11}^{W_3} &= \begin{pmatrix} 312(d+1) & 156(d+1) & 78(d+4) & 1248(d+1) \\ 156(d+1) & 39(5d+2) & 156(d+1) & 624(d+1) \\ 78(d+4) & 156(d+1) & 312(d+1) & 312(d+4) \\ 1248(d+1) & 624(d+1) & 312(d+4) & 1664(d+3)(d+1) \end{pmatrix} , \\
\mathcal{M}_{12}^{W_3} &= \begin{pmatrix} 624(d+1) & 312(d+2) & 156(d+4) & 624(d+1) \\ 312(2d+1) & 156(3d+2) & 312(d+1) & 312(d+1) \\ 156(3d+4) & 624(d+1) & 624(d+1) & 156(d+4) \\ 832(d+3)(d+1) & 416(d+6)(d+1) & 208(d+12)(d+1) & 832(d+3)(d+1) \end{pmatrix} , \\
\mathcal{M}_{13}^{W_3} &= \begin{pmatrix} 624(d+1) & 156(3d+4) & 312(d+4) \\ 156(3d+2) & 312(2d+1) & 624(d+1) \\ 312(d+2) & 624(d+1) & 1248(d+1) \\ 416(d+6)(d+1) & 208(d+12)(d+1) & 104(d^2+22d+48) \end{pmatrix} , \\
\mathcal{M}_{21}^{W_3} &= \begin{pmatrix} 624(d+1) & 312(2d+1) & 156(3d+4) & 832(d+3)(d+1) \\ 312(d+2) & 156(3d+2) & 624(d+1) & 416(d+6)(d+1) \\ 156(d+4) & 312(d+1) & 624(d+1) & 208(d+12)(d+1) \\ 624(d+1) & 312(d+1) & 156(d+4) & 832(d+3)(d+1) \end{pmatrix} , \\
\mathcal{M}_{22}^{W_3} &= (d+1) \begin{pmatrix} 416(2d+3) & 624(d+2) & 104\frac{(4d^2+25d+12)}{(d+1)} & 416(d+3) \\ 624(d+2) & 208\frac{(4d^2+7d+6)}{(d+1)} & 416(2d+3) & 208(d+6) \\ 104\frac{(4d^2+25d+12)}{(d+1)} & 416(2d+3) & 416(4d+3) & 104(d+12) \\ 416(d+3) & 208(d+6) & 104(d+12) & 416(4d+3) \end{pmatrix} , \\
\mathcal{M}_{23}^{W_3} &= \begin{pmatrix} 416(d+3)(d+1) & 312(d^2+7d+4) & 208(d+12)(d+1) \\ 312(d+2)^2 & 416(d+3)(d+1) & 416(d+6)(d+1) \\ 208(d+6)(d+1) & 416(d+3)(d+1) & 832(d+3)(d+1) \\ 416(2d+3)(d+1) & 104(4d^2+25d+12) & 208(d+12)(d+1) \end{pmatrix} , \\
\mathcal{M}_{31}^{W_3} &= \begin{pmatrix} 624(d+1) & 156(3d+2) & 312(d+2) & 416(d+6)(d+1) \\ 156(3d+4) & 312(2d+1) & 624(d+1) & 208(d+12)(d+1) \\ 312(d+4) & 624(d+1) & 1248(d+1) & 104(d^2+22d+48) \end{pmatrix} , \\
\mathcal{M}_{32}^{W_3} &= \begin{pmatrix} 416(d+3)(d+1) & 312(d+2)^2 & 208(d+6)(d+1) & 416(2d+3)(d+1) \\ 312(d^2+7d+4) & 416(d+3)(d+1) & 416(d+3)(d+1) & 104(4d^2+25d+12) \\ 208(d+12)(d+1) & 416(d+6)(d+1) & 832(d+3)(d+1) & 208(d+12)(d+1) \end{pmatrix} , \\
\mathcal{M}_{33}^{W_3} &= \begin{pmatrix} 208(4d^2+7d+6) & 624(d+2)(d+1) & 416(d+6)(d+1) \\ 624(d+2)(d+1) & 416(2d+3)(d+1) & 832(d+3)(d+1) \\ 416(d+6)(d+1) & 832(d+3)(d+1) & 1664(d+3)(d+1) \end{pmatrix} .
\end{aligned} \tag{A.10}$$

References.

- [1] D.J. Gross & F.J. Wilczek, Phys. Rev. **D9** (1974), 980.
- [2] E.G. Floratos, D.A. Ross & C.T. Sachrajda, Nucl. Phys. **B129** (1977), 66; **B139** (1978), 545(E).
- [3] E.G. Floratos, D.A. Ross & C.T. Sachrajda, Nucl. Phys. **B152** (1979), 493.
- [4] S. Moch, J.A.M. Vermaseren & A. Vogt, Nucl. Phys. **B688** (2004), 101.
- [5] S. Moch, J.A.M. Vermaseren & A. Vogt, Nucl. Phys. **B691** (2004), 129.
- [6] S. Moch, J.A.M. Vermaseren & A. Vogt, Nucl. Phys. Proc. Suppl. **135** (2004), 137.
- [7] S. Moch, J.A.M. Vermaseren & A. Vogt, Phys. Lett. **B606** (2005), 123.
- [8] M. Göckeler, R. Horsley, D. Pleiter, P.E.L. Rakow, A. Schäfer and G. Schierholz, Nucl. Phys. Proc. Suppl. **119** (2003), 32.
- [9] M. Göckeler, R. Horsley, H. Oelrich, H. Perlt, D. Petters, P.E.L. Rakow, A. Schäfer, G. Schierholz & A. Schiller, Nucl. Phys. **B544** (1999), 699.
- [10] S. Capitani, M. Göckeler, R. Horsley, H. Perlt, P.E.L. Rakow, G. Schierholz & A. Schiller, Nucl. Phys. **B593** (2001), 183.
- [11] C. Gattringer, M. Göckeler, P. Huber & C.B. Lang, Nucl. Phys. **B694** (2004), 170.
- [12] M. Göckeler, R. Horsley, D. Pleiter, P.E.L. Rakow & G. Schierholz, Phys. Rev. **D71** (2005), 114511.
- [13] M. Gürler, R. Horsley, P.E.L. Rakow, C.J. Roberts, G. Schierholz & T. Streuer, PoS LAT2005 **125** (2006), 124.
- [14] M. Göckeler, R. Horsley, Y. Nakamura, H. Perlt, D. Pleiter, P.E.L. Rakow, G. Schierholz, A. Schiller, H. Stüben & J.M. Zanotti, arXiv: 1003.5756 [hep-lat].
- [15] J.B. Zhang, D.B. Leinweber, K.F. Liu & A.G. Williams, Nucl. Phys. Proc. Suppl. **128** (2004), 240.
- [16] D. Bećirević, V. Gimenez, V. Lubicz, G. Martinelli, M. Papinutto & J. Reyes, JHEP **0408** (2004), 022.
- [17] J.B. Zhang, N. Mathur, S.J. Dong, T. Draper, I. Horvath, F.X. Lee, D.B. Leinweber, K.F. Liu & A.G. Williams, Phys. Rev. **D72** (2005), 114509.
- [18] F. Di Renzo, A. Mantovi, V. Miccio, C. Torrero & L. Scorzato, PoS LAT2005 (2006), 237.
- [19] V. Gimenez, L. Giusti, F. Rapuano & M. Talevi, Nucl. Phys. **B531** (1998), 429.
- [20] L. Giusti, S. Petrarca, B. Taglienti & N. Tantalo, Phys. Lett. **B541** (2002), 350.
- [21] A. Skouroupathis & H. Panagopoulos, Phys. Rev. **D79** (2009), 094508.
- [22] M. Constantinou, P. Dimopoulos, R. Frezzotti, G. Herdoiza, K. Jansen, V. Lubicz, H. Panagopoulos, G.C. Rossi, S. Simula, F. Stylianou & A. Vladikas, JHEP **1008** (2010), 068.

- [23] C. Alexandrou, M. Constantinou, T. Korzec, H. Panagopoulos & F. Stylianou, arXiv:1006.1920 [hep-lat].
- [24] R. Arthur & P.A. Boyle, arXiv:1006.0422 [hep-lat].
- [25] G. Martinelli, C. Pittori, C.T. Sachrajda, M. Testa & A. Vladikas, Nucl. Phys. **B445** (1995), 81.
- [26] E. Franco & V. Lubicz, Nucl. Phys. **B531** (1998), 641
- [27] K.G. Chetyrkin & A. Rétey, Nucl. Phys. **B583** (2000), 3.
- [28] J.A. Gracey, Nucl. Phys. **B662** (2003), 247.
- [29] J.A. Gracey, Nucl. Phys. **B667** (2003), 242.
- [30] J.A. Gracey, JHEP **0610** (2006), 040.
- [31] S.G. Gorishny, S.A. Larin, L.R. Surguladze & F.K. Tkachov, Comput. Phys. Commun. **55** (1989), 381.
- [32] S.A. Larin, F.V. Tkachov & J.A.M. Vermaseren, “The Form version of Mincer”, NIKHEF-H-91-18.
- [33] C. Sturm, Y. Aoki, N.H. Christ, T. Izubuchi, C.T.C. Sachrajda & A. Soni, Phys. Rev. **D80** (2009), 014501.
- [34] M. Gorbahn & S. Jäger, arXiv:1004.3997 [hep-ph].
- [35] L.G. Almeida & C. Sturm, arXiv:1004.4613 [hep-ph].
- [36] J.A. Gracey, JHEP **0904** (2009), 127.
- [37] S.A. Larin & J.A.M. Vermaseren, Phys. Lett. **B303** (1993), 334.
- [38] J.A.M. Vermaseren, math-ph/0010025.
- [39] P. Nogueira, J. Comput. Phys. **105** (1993), 279.
- [40] A.I. Davydychev, J. Phys. **A25** (1992), 5587.
- [41] J.C. Collins, *Renormalization* (Cambridge University Press, 1984).